Check for updates

# Processing polymer film nanocomposites of poly(vinylidene fluoride)/poly(ethylene oxide) and cobalt oxide nanoparticles for flexible energy storage systems

Ebtesam M. Alharbi[1] · A. Rajeh[2]

## Abstract

Using the solution cast method, researchers prepared Poly(vinylidene fluoride) (PVDF)/Poly(ethylene oxide) (PEO) blend doped with various weight ratios of Cobalt oxide nanoparticles ($Co_3O_4$ NPs). XRD analysis revealed a remarkable increase in the amorphous nature of the nanocomposites as the $Co_3O_4$ concentration climbed. The Notable alterations were revealed by the FT-IR spectra, revealing interactions between the PVDF/PEO blend and $Co_3O_4$ NPs. We found a significant red shift in the fundamental absorption edge of nanocomposites films using UV–visible spectroscopy. As the concentration of $Co_3O_4$ ions rose, the direct bandgap of PVDF/PEO film decreased significantly, from 5.39 eV to 3.96 eV, while the Urbach energy increased. Thermal analysis in the range of 30–500 °C revealed a remarkable improvement in the thermal stability of the nanocomposites compared to their pure PVDF/PEO blend. The endothermic melting temperature ($T_m$) of the PVDF/PEO blend is 130 °C was calculated from DSC analysis. To delve into the electrical behavior of the films, its conductivity was examined using an AC impedance analyzer over a broad frequency range of 100 Hz–7 MHz at room temperature. As the $Co_3O_4$ NP content ramped up and the frequency climbed, the material's electrical conductivity responded in kind, showing a consistent upward trend. The electrical conductivity of the nanocomposite films, as a function of frequency, neatly follows Jonscher's equation. The PVDF/PEO blend containing 2%$Co_3O_4$ NPs reigned supreme in terms of ionic conductivity, boasting a remarkable $6.5 \times 10^{-4}$ $Scm^{-1}$ at room temperature. The dielectric constant increases with $Co_3O_4$ concentration, according to dielectric permittivity studies, because of interfacial polarization at the PVDF/PEO and $Co_3O_4$ interfaces. The findings show that the films made from nanocomposites have improved optical, thermal, electrical, and dielectric properties. The gathered data suggests that the $Co_3O_4$ nanoparticles doped PVDF/PEO mix films are a novel, easy-to-work-with, and promising material for a range of applications, such as optoelectronics, electronics, and other flexible energy storage devices.

**Keywords** PVDF/PEO/$Co_3O_4$ nanocomposites · Optical properties · Thermal properties · AC conductivity · Dielectric parameters

---

Extended author information available on the last page of the article

# 1 Introduction

Polar polymer blends (PBs) that are miscible and compatible are recognized as efficient host matrix for the creation of innovative polymer nanocomposites (PNCs) materials, which are employed in cutting-edge flexible device technologies (Deeba et al. 2022; Sengwa et al. 2023; Al-Sulami et al. 2024). By combining various polymer qualities with cutting-edge technology, several commercializable thermophysical properties, including mechanical, thermal, structural, dielectric, chemical, and optical, can be tuned or modified (Formela et al. 2016). Furthermore, blending polymers to create suitable novel polymeric materials is a green chemistry approach that is favored over synthesizing the new polymer through dangerous chemical reactions. PNCs materials with promising qualities have so far been thoroughly investigated for their applicability in the development of high performance devices, mostly in the fields of medical technology, microelectronics, opto-electronics, sensors, actuators, energy harvesters, energy storage, heat insulators and electromagnetic interference shielders (Xia et al. 2022; Ravisankar et al. 2023). New materials, including blends and composites, are making a significant contribution to a wide range of scientific disciplines, both from a technological and scientific standpoint. Semi-crystalline polymer poly(vinylidene fluoride) (PVDF) has many uses because of its exceptional qualities, which include strong mechanical strength, resistance to harsh chemicals, and remarkable thermal stability (Rajabzadeh et al. 2009). Additionally, PVDF has been extensively researched due to its impact on the creation of electronic devices, as well as its rather good pyroelectric and piezoelectric response and polymorphic forms (Chu, et al. 2023). Infrared imaging, transducers, piezoelectric sensors, and other military and biological domains all make extensive use of PVDF (Rajeh et al. 2023). PVDF is more flexible and has better electrical qualities than traditional materials. It is also easier to prepare at low temperatures (Dallaev et al. 2022). Many pairs of blends have been studied, such as PVDF/PVP (Panwar et al. 2012), PVDF/PVAc (Baskaran et al. 2006), and PVDF/PMMA (Abdelaziz 2013), due to PVDF's high miscibility with oxygen-containing polymers (Panwar et al. 2012), which is related to the interaction between the partner's carbonyl groups and fluorine atoms. In contrast, over fifty years, a great deal of research has been conducted on Poly(ethylene oxide) (PEO), the first-creation polymer employed as a host matrix for the creation of PNCs (Long et al. 2016; Wan et al. 2018). Because of its good flexible type film forming ability by melt pressing and solution cast, low cost, high stability towards reduction, and relatively easy handling and processing, the PEO matrix continues to be the first choice of researchers when developing novel PNCs. However, its main drawbacks are a low mechanical strength and high degree of crystallinity (Morsi et al. 2019; Alzahrani et al. 2022; Alsulami and Rajeh 2021). The blending of PEO and PVDF produces an enhanced and tunable thermomechanical properties blend matrix, which is of remarkable significance regarding the safer workability of PNCs with higher ionic conductivity. This is because the PVDF matrix has higher mechanical and thermal stabilities than the PEO matrix (Monaca et al. 2017; Xi et al. 2006). Additionally, the PVDF/PEO blend-based PNCs have relatively high dielectric constant and excellent electrochemical strength because of the strong functional group (-C-F) to the electron-withdrawing in the backbone of PVDF, which together facilitate filler dispersion and raise the ion density at the fixed filler concentration (Dhatarwal and Sengwa 2020a). These blend-based polymer blend PNCs have high porosity membranes, which helps to promote ion mobility (Prasanth et al. 2014). Based on its compatibility to form the blend with PEO (Appetecchi et al. 2003) and have strong thermal stability (Hema et al. 2009) PVDF is chosen. A prior work created

a polymer electrolyte for enhanced ionic conductivity at room temperature using PVDF/ PEO blend hosts (Patla et al. 2018). Also, the study of different composition wt% blends showed that the PVDF/PEO blend $\cong$ 80/20 wt% has been suggested for the synthesis of lithium-ion conducting solid polymer electrolyte due to its good plasticity, almost homogeneous character, good blending, and predominantly presence of PEO in an amorphous phase (Xi et al. 2006; Dhatarwal and Sengwa 2020a). To better understand the electrochemical properties of PNCs, reports have been made on the inclusion of metal oxides such as titania($TiO_2$) (Wang and Kim 2007), $BaTiO_3$ (Kułek et al. 2007), and various lithium salts (Bhatt and Bhat 2012; Shen et al. 2004). Few others have reported $Co_3O_4$/PANI PNCs as electrode materials for super-capacitors (Ren et al. 2018), $Co/Co_3O_4$ nanocomposite for hybrid super-capacitors (Zhang et al. 2020), $Co_3O_4$/polypyrrole nanocomposite for super-capacitors (Ma et al. 2018), $Co_3O_4$/CMC/PVA films are a potential option for several industrial and electronic applications, because of their increased charge storage capacity and dielectric strength (Sayed and El-Gamal 2015), and $Ag/Co_2O_3$-PVP/CS polymer nanocomposites are a good option for energy storage devices and optoelectronic applications (Ragab et al. 2024), etc. $Co_3O_4$ nanoparticles will affect the dielectric permittivity of the $Co_3O_4$-CMC/PVA system since their permittivity value is higher than that of pure polymer (Sayed and El-Gamal 2015). Nonetheless, research hasn't been done on the thermal, optical, conductivity, and dielectric properties of cobalt oxide ($Co_3O_4$) nanoparticles on PVDF/ PEO matrix. It will be interesting to see how the characteristics of PVDF/PEO and $Co_3O_4$ nanoparticles combine. The $Co_3O_4$, on the other hand, is a metal oxide that is a member of the family of ferrites that resemble spinel. Spinel ferrites exhibit considerable promise in resistive switching, memory, microwave, and magneto-electric coupling devices (Al-Gharram and AlZoubi 2024). $Co_3O_4$ NPs can therefore improve dielectric and optical properties (Ragab et al. 2024; Al-Gharram and AlZoubi 2024). To obtain innovative properties, our study suggests a hybrid PVDF/PEO and $Co_3O_4$ NPs nanocomposite. To enhance the optical, thermal, electrical, and dielectric properties, however, better nanoparticle dispersion and more interfacial interaction between the nanomaterial and PVDF/PEO blend are required. The $Co_3O_4$-PVDF/PEO nanocomposites films were prepared using the solution casting approach. This study is the first to look at how $Co_3O_4$NPs affect the physical characteristics of a PVDF/PEO blend, according to the literature. Lastly, an assessment was conducted on the $Co_3O_4$NPs dispersion properties within the PVDF/PEO matrix. These hybrid nanocomposites are a great option for many to be applied in a variety of applications due to their improved optical, thermal, dielectric, and electrical properties.

## 2 Experimental work

### 2.1 Materials

PVDF (MW = 534,000) was obtained from Sigma Aldrich Pvt. Ltd. Purchased from ACROS, New Jersey, USA, the PEO powder with Mw = 40,000 $gmol^{-1}$. The $Co_3O_4$ NPs was obtained from Sigma Aldrich. MERCK provided the solvent N, N Dimethylformamide (DMF, 99.5%).
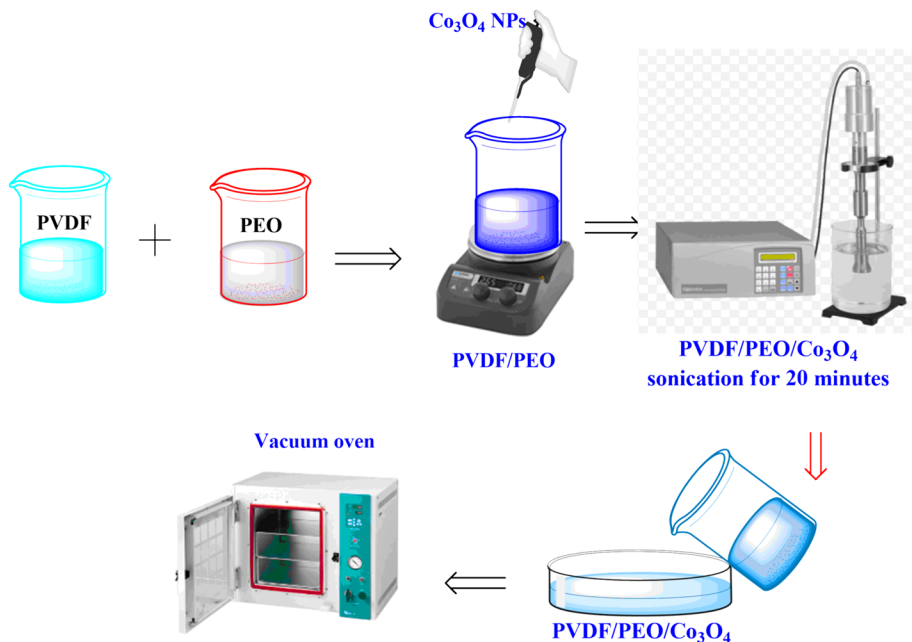
**Scheme 1** Experimental representative of preparation processes of PVDF/PEO/Co$_3$O$_4$ PNCs

## 2.2 Preparation of PVDF/PEO-Co$_3$O$_4$ PNCs

PVDF/PEO/Co$_3$O$_4$ polymer nanocomposites were created via the solution casting technique. Before being used to prepare films, PEO, PVDF, and Co$_3$O$_4$ NPs were vacuum-dried at the proper temperature. To make PNCs films with various concentrations of Co$_3$O$_4$, first, the appropriate contents of PVDF and PEO for the PVDF&PEO blend = 80/20 wt%/wt% were taken, and these were dissolved in the solvent of DMF at 75 °C with a magnetic stirrer until the mixture (80PVDF/20PEO blend) became clear and homogenous. Following that, the appropriate concentrations of Co$_3$O$_4$ NPs for xwt% (x = 0.1, 0.5, 1.5, and 2.0) were added to the relevant polymeric solutions. To fully distribute the Co$_3$O$_4$NPs, each solution was then aggressively magnetically agitated once more while being heated to a moderate temperature. A magnetic stirrer and prob sonicator were used to agitate the solution for an hour to produce a homogeneous mixture and good dispersion of the nanoparticles. Each combination is put in a glass Petri dish and left to evaporate slowly inside a vacuum oven at 80 °C. The films employed for characterization varied in thickness from 0.15 to 0.3 mm (Scheme 1).

## 2.3 Measurements tools

The samples that had previously been made were subjected to structural characterization by X-ray diffraction (X'pert PROPAN analytical). The Co$_3$O$_4$ NPs were investigated utilizing transmission electron microscopy(TEM, JEM 2100, Jeol, Japan) to determine their average size, morphology, and shape. The Fourier transform infrared (FTIR) spectra of

the pure blend and PNCs samples were acquired using FTIR-430, JASCO Japan in the 4000–500 $cm^{-1}$ to identify potential interactions in the product films. With an accelerating voltage of 20 kV, the surface morphology of the nanocomposites films was examined using a scanning electron microscope (JEOLJSM-6510LV, USA). The UV–Vis spectrophotometer (Jasco V-630, Japan) was used to measure the UV–Vis absorption spectra between 190 and 1000 nm. With different loadings of $Co_3O_4$ NPs, the thermal stability of the pure blend was assessed using a thermogravimetric analyzer (STD-Q600, USA). The dielectric data and the AC conductivity were obtained using Quatro temperature controls in conjunction with broadband dielectric spectroscopy (Novocontrol Turnkey Concept 40 System).

# 3 Results and discussion

## 3.1 XRD and TEM

When it comes to unraveling the intricate connection between structure and properties in polymer nanocomposites, X-ray diffraction spectroscopy reigns supreme. As seen in Fig. 1, XRD measurements were made to look into the crystal structures of $Co_3O_4$ NPs, PVDF/PEO, and PVDF/PEO/$Co_3O_4$ films. The $Co_3O_4$ NPs (Fig. 1a) displayed at 2θ in the of 31.32°; 36.92; 38.82°; 42.58°; 44.78°; 55.48°; 59.89° and 65.26°. These peaks correspond to the (022), (311), (222), (040), (400), (133), (511), and (044), planes of cobalt oxide crystals, respectively. The stated values (COD data of $Co_3O_4$ 96-153-8532) have been matched with these diffraction peaks. No peaks that could have been caused by impurities were found. This XRD result showed strong consistency with previous research (Saeed et al. 2022). Using the Debye-Scherer equation, the particle size of $Co_3O_4$ NPs was approximately 14.75 nm. According to Fig. 1b, the TEM picture revealed that the morphology of the $Co_3O_4$ NPs was spherical, with an average size of 5–20 nm (Fig. 1b). This outcome is consistent with the literature (Saeed Farhadi and Javanmard 2016). A pure PVDF/PEO blend appears to be semi-crystalline, based on the Fig. 1c. The pure PVDF/PEO blend film's XRD pattern showed diffraction peaks at 2θ=20.62° and 39.92°, which corresponded to the PVDF crystallites (*hkl*) planes (110/200) and (201/111), respectively, and explained the polymer blend's multiphase semicrystalline character (Wan et al. 2022; Dhatarwal and Sengwa 2020b). The diffraction peaks seen at 20.62° and 39.92° represent electro-active polar β-phase crystals, and there is a chance that these crystals may have combined with α-phase crystals (Sengwa et al. 2023; Meng et al. 2010). A few changes in the PVDF/PEO- $Co_3O_4$ nanocomposites' peak positions relative to the pure $Co_3O_4$ nanopowder and pristine PVDF/PEO film, respectively, show that interaction between the polymer chains and the $Co_3O_4$ NPs have been established. The appearance of all the $Co_3O_4$ peaks indicates that the $Co_3O_4$ nanoparticles in these synthesized polymer nanocomposite materials have not changed in crystalline shape, aside from the presence of polymer-nanoparticle interaction (Sengwa et al. 2023). Moreover, as shown in Fig. 1c, the peak intensities of the different $Co_3O_4$ crystallites in the PNCs films grow linearly to 2 weight percent of nanofiller. This discovery elucidates the highly homogeneous dispersion of nanoparticles within the PVDF/PEO polymer mix matrix, and the superior nanocomposites, as evidenced by comparable outcomes observed in several other PNCs materials (Sengwa et al. 2019; Sengwa and Dhatarwal 2021; Choudhary and Sengwa 2018). The area under the crystalline peaks divided by the total area was utilized to calculate the samples' degree of crystallinity. Table 1 lists the crystallinity values that were achieved for the pure PVDF/PEO and
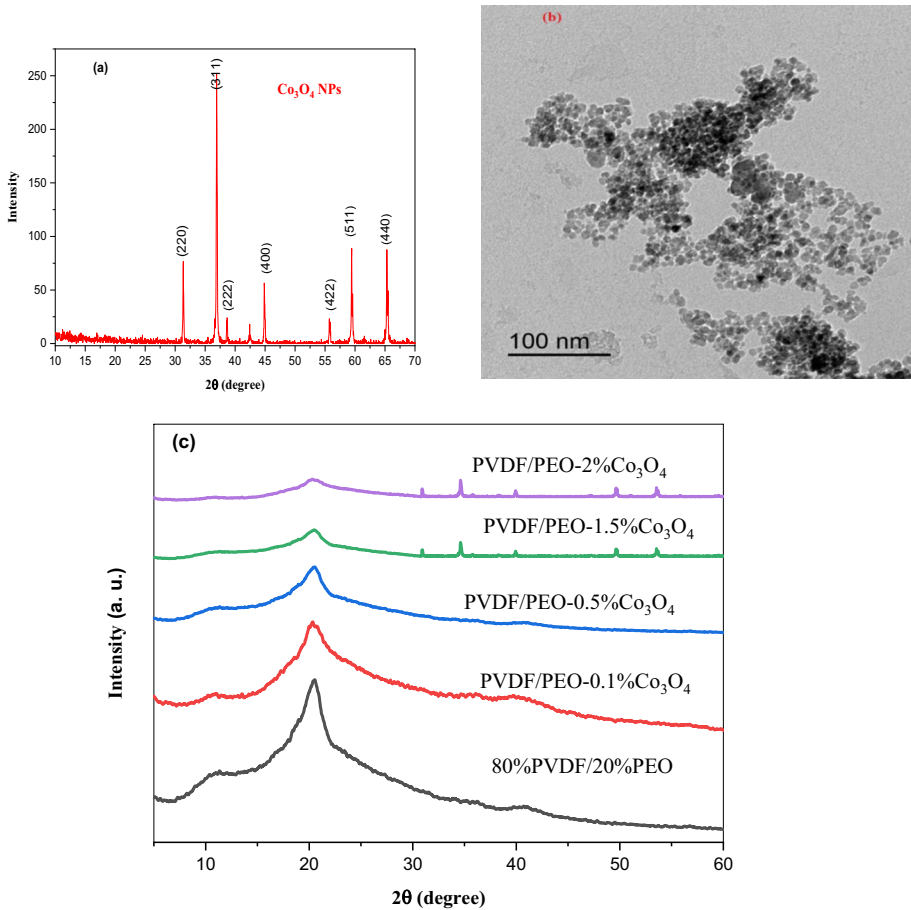
**Fig. 1 a** XRD pattern of pure $Co_3O_4$, **b** TEM of pure $Co_3O_4$, and **c** XRD pattern of PVDF/PEO blend and PNCs at different contents of $Co_3O_4$

**Table 1** Data of Eg (direct and indirect), $E_U$, Xc, relaxation time (s) and $\sigma_{dc}$ for pure PVDF/PEO and PNCs at different contents of $Co_3O_4$ NPs

| Samples | $E_{g\ indirect}$ | $E_{g\ direct}$ | $E_U$ | Xc (%) | Relaxation time (s) | $\sigma_{dc}$ (Scm$^{-1}$) |
|---|---|---|---|---|---|---|
| PVDF/PEO blend | 5.11 | 5.39 | $0.1879 \pm 0.021$ | 37.24 | 0.854 | $5.5 \times 10^{-9}$ |
| PVDF/PEO/0.1%$Co_3O_4$ | 4.65 | 5.01 | $0.1978 \pm 0.001$ | 30.94 | 0.759 | $3.5 \times 10^{-8}$ |
| PVDF/PEO/0.5%$Co_3O_4$ | 4.35 | 4.86 | $0.2341 \pm 0.012$ | 23.43 | 0.369 | $2.3 \times 10^{-7}$ |
| PVDF/PEO/1.5%$Co_3O_4$ | 3.96 | 4.56 | $0.2562 \pm 0.032$ | 19.78 | 0.285 | $1.1 \times 10^{-5}$ |
| PVDF/PEO/2%$Co_3O_4$ | 3.61 | 3.96 | $0.2745 \pm 0.002$ | 15.10 | 0.210 | $3.5 \times 10^{-5}$ |

PVDF/PEO/ $Co_3O_4$ nanocomposites. At 2 wt% $Co_3O_4$ loading, the crystallinity degree ($\chi c$) drops to 15.10 from around 37.24% for pure PVDF/PEO. Generally, the polymer and kind of nanofiller utilized to determine how crystallinity varies in polymer nanocomposites.

The remarkable polymer/nanofiller interfacial properties can change the crystallinity by decreasing or increasing (Boranna et al. 2023). The inclusion of $Co_3O_4$ nanoparticles in the current work increased the structural disorder of the PVDF/PEO/$Co_3O_4$ nanocomposites. The presence of interactions between nanoparticles and the side chain of PVDF/PEO polymer impairs the crystallization when they are added to the polymer matrix. The microstructure of polymeric chains is disrupted and the amorphous phase in polymer nanocomposites is facilitated by the interaction between nanoparticles and the polymer matrix (Ningaraju and Ravikumar 2017). Changes in the organization or conformation of polymer chains within the PVDF/PEO matrix could be the cause of the weakening of crystallinity upon the addition of $Co_3O_4$ nanoparticles (Kim et al. 2013; Dey et al. 2011).

## 3.2 FTIR analysis

The significant interaction between $Co_3O_4$ NPs and the PVDF/PEO matrix was further demonstrated by FTIR spectroscopy, and the resulting nanocomposites spectrum is displayed in Fig. 2. From FTIR spectra, we noticed the two absorption bands positions at 2989 and 2868 cm$^{-1}$ verify the existence of the symmetric $CH_2$ and the asymmetric vibration (Mohammed et al. 2018). According to earlier research (Dhatarwal and Sengwa 2020a; Pradeepa et al. 2016), the band at 1420 cm$^{-1}$ for PVDF/PEO correlates to the wagging modes of $CH_2$, while the band at 1271 cm$^{-1}$ is associated with the $CH_2$ twisting mode of PEO. The stretching mode of PVDF's $CF_2$ is responsible for the band at 1176 cm$^{-1}$. The band at 1083 cm$^{-1}$ was consistent with PEO's C–O stretching mode. Additionally, we detected a band at 845 cm$^{-1}$ that is indicative of a combined mode of $CH_2$ rocking and $CF_2$ asymmetric stretching vibration. The C–$F_2$ bending vibration is detected at 675 cm$^{-1}$. The vibrational peaks at 560 cm$^{-1}$ are responsible for the bending and wagging vibrations of $CF_2$. Several notable alterations were noticed in the vibrational modes of the PVDF/PEO blend as the concentration of $Co_3O_4$ NPs increased. The $CF_2$ band at 1176 cm$^{-1}$ shifted to a lower wavenumber, while the bands at 1420 cm$^{-1}$ and 1083 cm$^{-1}$ showed a shift towards a longer wavenumber. Changes in vibrational modes were indicated by the band's disappearance at 560 cm$^{-1}$. Additionally, as the concentration of $Co_3O_4$ NPs increased, the intensities of several bands dropped, indicating the formation of complexes and interaction between PVDF/PEO and $Co_3O_4$ NPs. The comparison study revealed that, for these nanocomposites, there is a discernible change in the position and form of the infrared bands and a drop in band intensity with increasing $Co_3O_4$ nanoparticle concentration. It is clear from the data analysis that the functional groups of the PVDF/PEO and the $Co_3O_4$ nanoparticles interact physically, as seen in Scheme 2 (Ouyang et al. 2015). Nanocomposite materials that contain dispersed nanoparticles can physically confine polymer chains, leading to changes in the molecular packing of the polymers. This results in pronounced changes in the crystalline structures, as indicated in previous literature on other nanocomposite (Sengwa et al. 2020).

## 3.3 SEM analysis

SEM is a technique that has been studied to gain deeper insights into the structural modifications of the nanocomposites samples. The SEM pictures show the variations in the concentrations of $Co_3O_4$ NPs have been incorporated. The SEM images of the PVDF/PEO-$Co_3O_4$ nanocomposite films are displayed in Fig. 3a–e. The blend film's fingerprint-shaped, smooth surface was noticed, confirming its homogeneous composition and don't
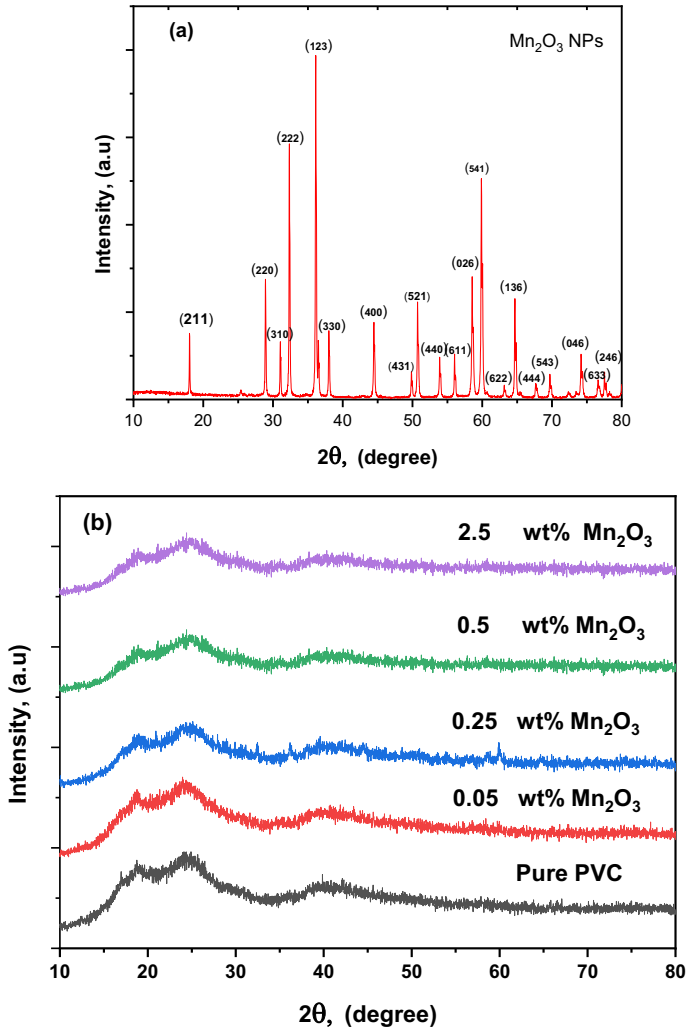
**Fig. 2** FTIR spectra of PVDF/PEO blend and PVDF/PEO-Co$_3$O$_4$ PNCs

any phase separation between PVDF and PEO; in other words, they are miscible because it cannot be observed the boundaries between the PEO and PVDF phases (see Fig. 3a). This finding is in line with the findings of Ramesh et al. (Alsalmah et al. 2024a). Additionally, the pure PVDF/PEO blend exhibits semi-crystalline behavior, and the smooth surface behavior found in the polymer matrix is advantageous for quick ionic transport (Alsalmah et al. 2024a). The morphology of blend polymer nanocomposites with varying nanoparticle concentrations in the polymer matrix is displayed in Fig. 3b–e. The complexation of the nanoparticles and polymer matrix is more than confirmed by the highly conductive polymer mix alterations in the crystalline-structure morphology (Alsalmah et al. 2024a). Consequently, the polymer–nanoparticles matrix's increased amorphous content and smooth shape encourage quicker ion transport (Alsalmah et al. 2024a; Ye et al. 2007). However, loading Co$_3$O$_4$ NPs causes the blend surface to become rougher (Fig. 3b–e). Observations
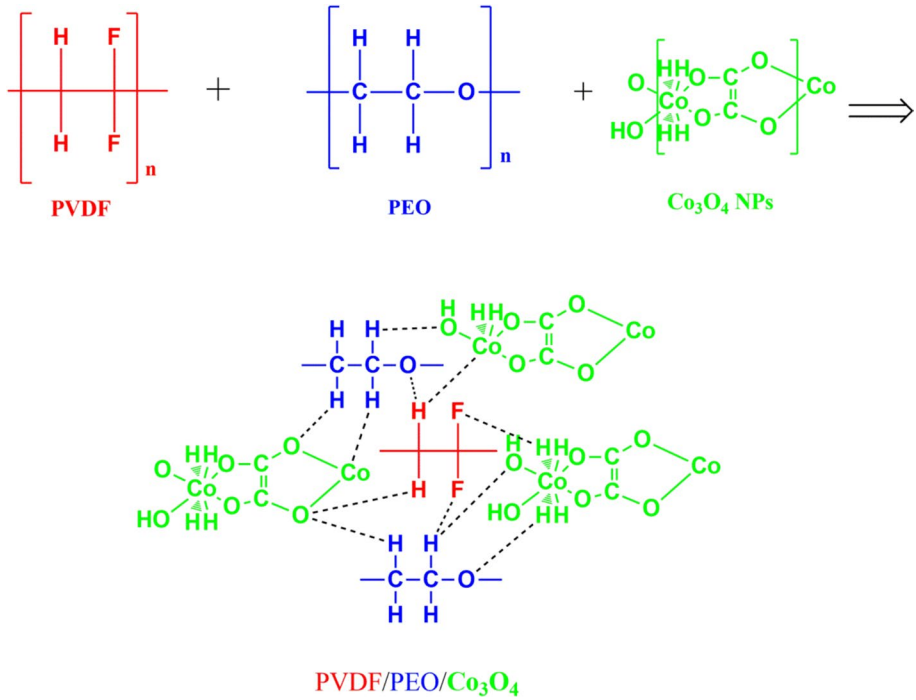
**Scheme 2** Shows the possible mechanism for interaction between of PEO, PVDF, and $Co_3O_4$ nanocomposites

of the white and black regions support the notion that $Co_3O_4$ is present in the white regions, while the black regions were for the polymer-rich. The optical, thermal, conductivity and dielectric properties of these PNCs are governed by the well-noted $Co_3O_4$ NP distribution, indicating strong compatibility between the $Co_3O_4$ and the blend matrix. It was discovered also that 2 wt%$Co_3O_4$ loaded film has the maximum number of particles compared to other loading ratios and there is some degree of agglomeration of $Co_3O_4$ NPs. As a result, the SEM results that were obtained agree with the findings of the XRD studies.

## 3.4 Optical absorption studies

### 3.4.1 Spectrum characterization

Optical absorption spectra can be used to reveal fundamental details about the electronic band structure of solids. Figure 4 shows the UV–visible optical absorption spectra of pure PVDF/PEO and $Co_3O_4$ NPs-doped PVDF/PEO films. The PVDF/PEO film shows a broad absorption band centered at 287 nm. The band can be attributed to a $\pi-\pi^*$ transition in unsaturated bonds, predominantly (C=C) (Kacem et al. 2023). Furthermore, the optical spectra of $Co_3O_4$-doped polymer blend films show that the absorption band maximum shifted to the higher wavelengths as the concentration of $Co_3O_4$ NPs increased. Additionally, when the concentration of $Co_3O_4$ rises, so does

Pure PVDF/PEO

PVDF/PE/0.1%Co$_3$O$_4$

PVDF/PE/0.5%Co$_3$O$_4$

PVDF/PE/1.5%Co$_3$O$_4$
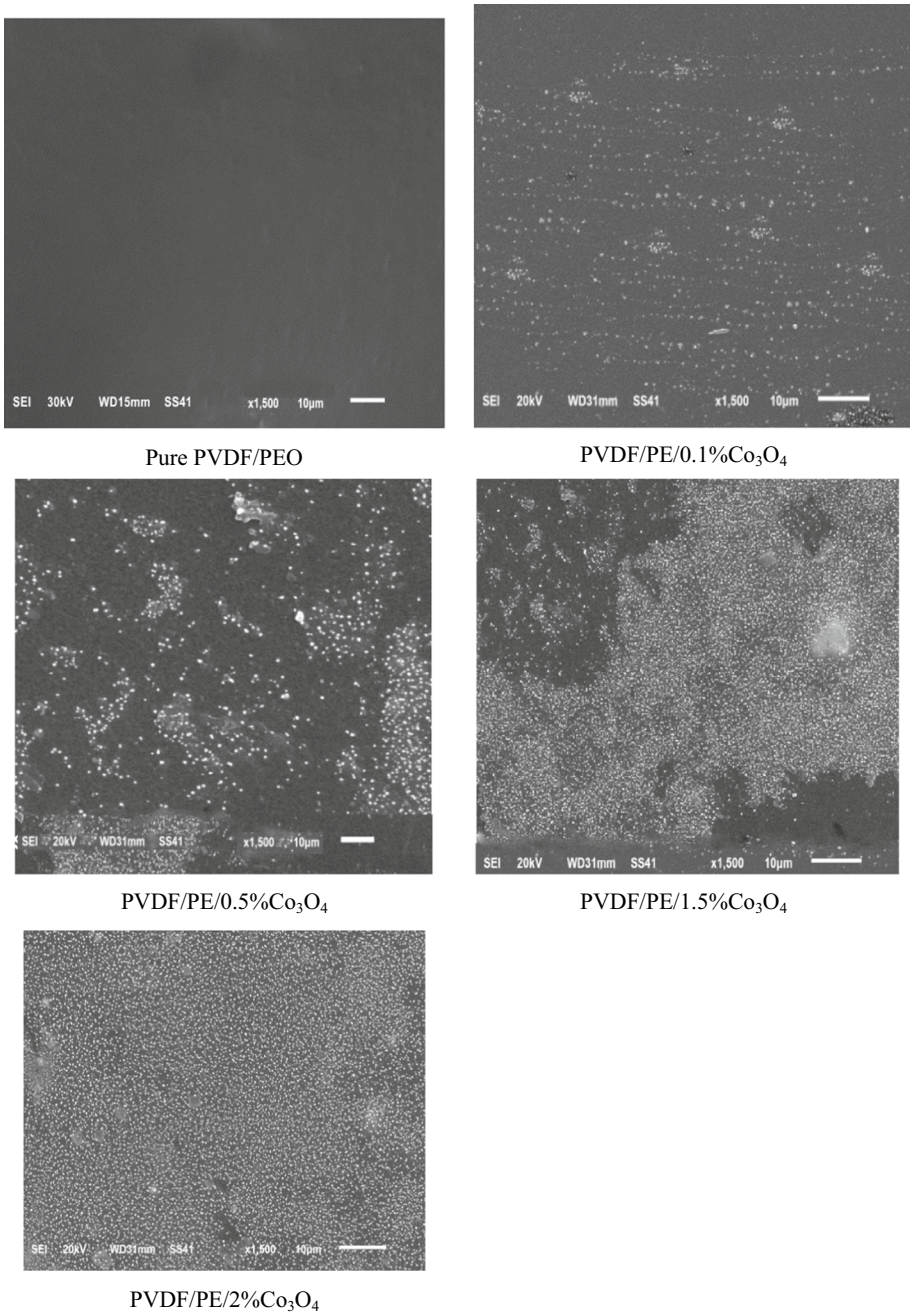
PVDF/PE/2%Co$_3$O$_4$

**Fig. 3** SEM micrographs of PVDF/PEO blend and PNCs at different contents of Co$_3$O$_4$ NPs
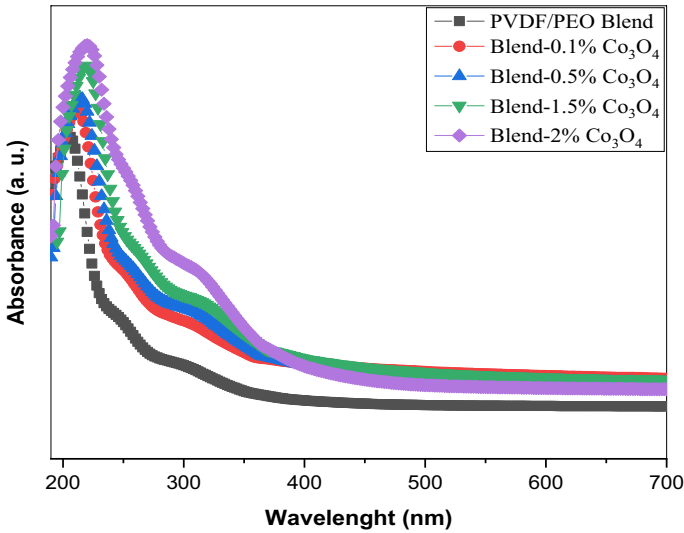
**Fig. 4** UV–Visible absorption spectra for PVDF/PEO blend and PNCs at different contents of $Co_3O_4$ NPs

the absorption, suggesting that, according to the effective mass approximation, the increase in absorbance is roughly proportionate to the concentration of $Co_3O_4$ (Alsalmah et al. 2024b).

### 3.4.2 Optical energy band gap (Eg)

Following the relationship expressed in Eqs. (1), and (2), the Eg of the samples was determined (Alghamdi and Rajeh 2023a; Alqarni et al. 2024):

$$(ahv) = A\left(hv - E_g\right)^{1/2} \qquad \text{indirect} \tag{1}$$

$$(ahv) = A\left(hv - E_g\right)^{2} \qquad \text{direct} \tag{2}$$

where, A is a constant, h$v$ is the photon energy, Eg is the optical band gap, and $\alpha$ is the absorption coefficient. The band gap plot of the $Co_3O_4$-PVDF/PEO nanocomposites films is displayed in Fig. 5a, b. The optical band gap values of PVDF/PEO blends doped with 2 wt% $Co_3O_4$ were determined by intercepting the $(\alpha hv)^2$ and $(\alpha hv)^{1/2}$ vs. h$v$ curves. The results, shown in Table 1, indicate a significant decrease in $E_{gdirect}$, from 5.39 eV for pure PVDF/PEO to 3.96 eV for the (2 wt%) doped blend. According to a studies, the optical properties of polymer nanocomposites may be impacted by modifications in their electronic structure (Almehmadi et al. 2023). The creation of new energy levels (traps) between the HOMO and LOMO as a result of the disorder building in the PNCs films is what causes the fall in Eg values. As a result, the density of localized states increases in the PVDF/PEO matrix's mobility band gap (Abdullah et al. 2016). The XRD data reinforce the creation of disorder in the PNCs films (Fig. 1).
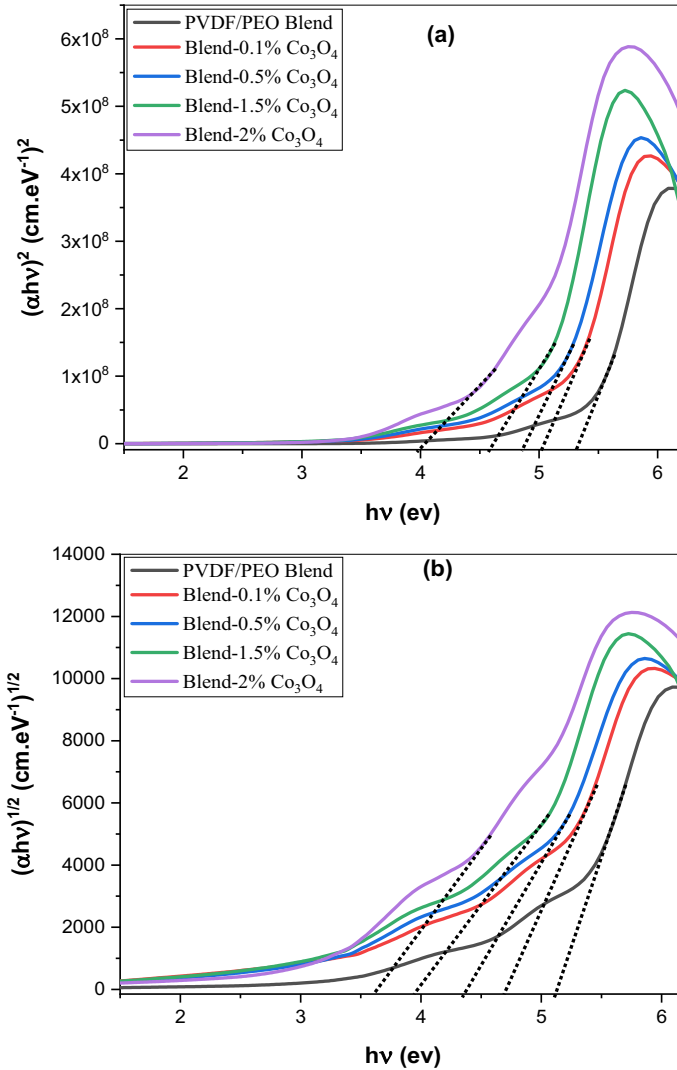
**Fig. 5** **a** $(\alpha h\nu)^2$ and **b** $(\alpha h\nu)^{1/2}$ versus $h\nu$ of PVDF/PEO blend and PNCs at different contents of $Co_3O_4$ NPs

### 3.4.3 Optical energy Urbach (EU)

In contrast, photon absorption for optical transitions resulting from photons with energy $h\nu$ < Eg will be associated with the existence of localized tail states within the forbidden gap. The Urbach tail's width serves as a barometer for the prohibited band gap's defect levels. The width of the Urbach tail was determined using the relation that follows (Alghamdi and Rajeh 2023b):
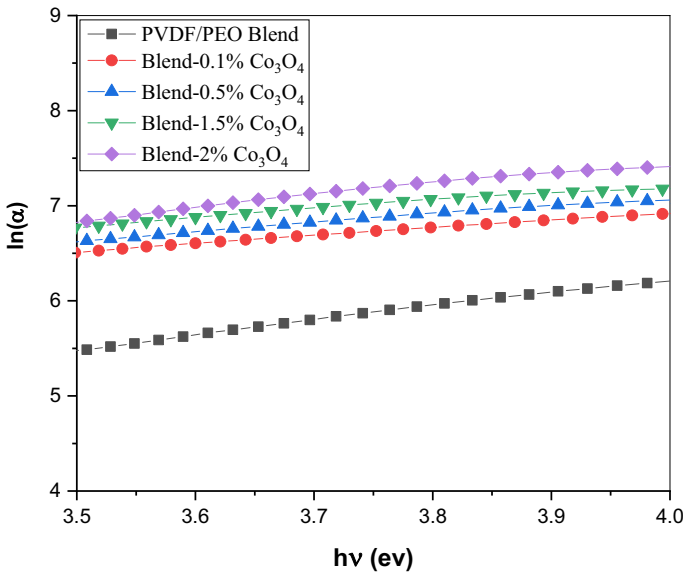
$$a = a_o \exp\left(h\nu/E_U\right) \tag{3}$$

**Fig. 6** Behaviour of $\ln(\alpha)$ versus h$v$ for pure blend and PNCs at various contents of $Co_3O_4$ NPs

where, $\alpha_o$ is constant and the slope of the straight lines of Ln $(\alpha)$ versus h$v$ is the Urbach tail $E_U$ as shown in Fig. 6. The values of the $E_U$ listed in Table 1. It is evident that when the content of $Co_3O_4$ NPs in the PVDF/PEO matrix rises, so do the $E_U$ values. This attests to an increase in both the localized states in the forbidden band gaps and the degree of disordering of the polymer film structure. Furthermore, transitions from band to tail and from tail to tail are more likely (Alsulami and Rajeh 2023).
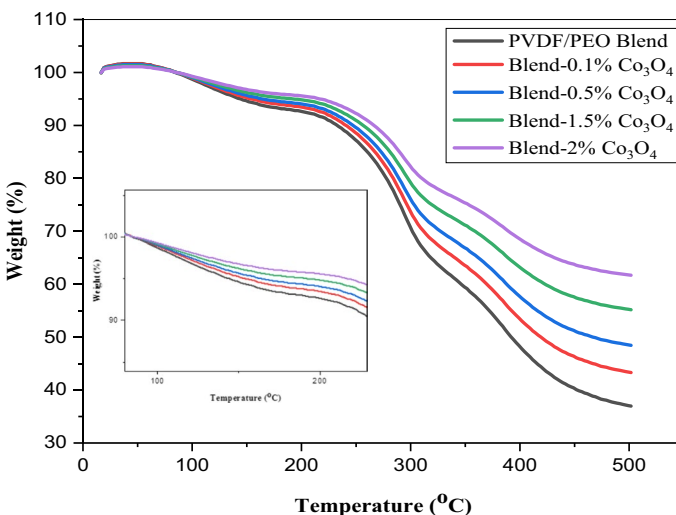


**Fig. 7** TGA patterns of the PVDF/PEO and PVDF/PEO-$Co_3O_4$ nanocomposites

## 3.5 Thermal degradation studies (TGA)

Figure 7 shows the blend with varying amounts of $Co_3O_4$ nanoparticles and the thermal stability of PVDF/PEO. Every sample displays three distinct phases of decomposition patterns. The elimination of solvent absorbed in the blend matrix causes the first stage of thermal degradation to occur between 50 and 150 °C. The first degradation temperature observed in thermogravimetric analysis (TGA) of PVDF is attributed to a chain stripping mechanism that occurs through the scission of C–H and C–F bonds. The breakdown of the compound results in the formation of a conjugated sequence, concurrently releasing hydrogen fluoride. At the final degradation temperature, these unstable polyenic sequences that were produced at the first degradation temperature degrade to char (Mukherjee and Dasgupta Ghosh 2023). The second thermal decomposition event observed between 238 and 350 °C can be ascribed to the melting of PVDF/PEO chains. Degradation of the remaining blend matrix occurs during the third stage of decomposition, which occurs between 360 and 475 °C. The final stage of decomposition occurs when the polymer chain degrades, which occurs between 330 and 450 °C (Alghamdi and Rajeh 2022). PVDF/PEO- $Co_3O_4$ nanocomposites are more stable than PVDF/PEO, according to the TGA data. The TGA data validate the interaction between PVDF/PEO and $Co_3O_4$ nanoparticles. The figure (as shown insert in Fig. 7) also shows that all of the nanocomposites films have greater decomposition temperatures than pure blend. Additionally, as the amount of $Co_3O_4$ nanoparticles in the mixed nanocomposite grows, so does its thermal stability. Improved thermal stability of the nanocomposite films is ascribed to the strong interfacial contacts between $Co_3O_4$ nanoparticles and the PVDF/PEO blend (Abdelrazek et al. 2023).
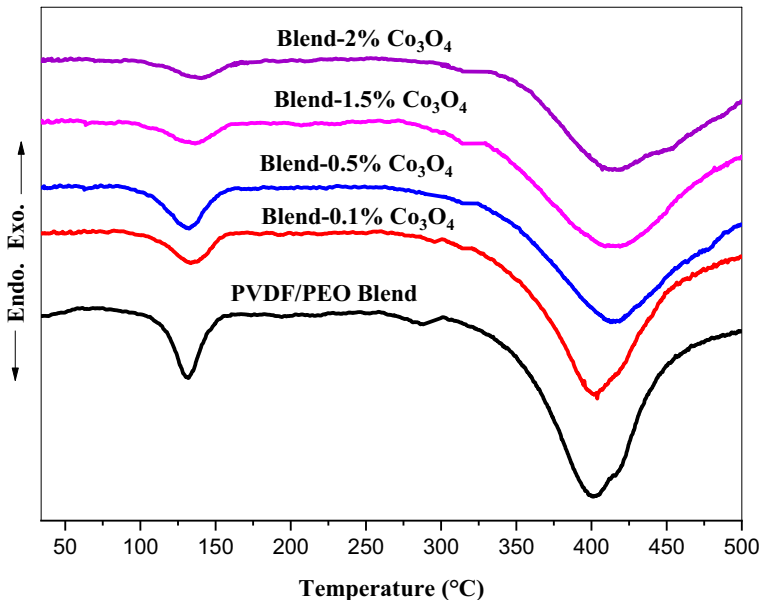


**Fig. 8** DSC thermograms of PVDF/PEO and PVDF/PEO doped with different contents of $Co_3O_4$ NPs

## 3.6 Differential scanning calorimetery (DSC)

DSC curves at 30–500 C were utilized to investigate the thermal behavior of the PVDF/PEO blend doped with $Co_3O_4$ NPs. Figure 8 displays the DSC data curve for each sample. Every sample's DSC curve has a distinct endothermic peak. The glass transition temperatures $T_g$ of pure PEO and PVDF, according to earlier studies, are −45 °C (Sengwa and Dhatarwal 2022) and −36 °C (Wang et al. 2022), respectively, which, in the current work, falls outside of the designated experimental temperature range. Additionally, some earlier research indicated that PVDF and PEO formed a miscible blend (Dhatarwal and Sengwa 2022), which is to be expected given that both polymers established strong hydrogen bond contacts, as shown by examining their FTIR spectra. The first endothermic melting temperature ($T_m$) of the PVDF/PEO blend is 130 °C, while the $T_m$ of the nanocomposite with 0.1, 0.5, 1.5, and 2 weight percent of $Co_3O_4$ NPs are centered at 133, 135, 140, and 143 °C respectively. The crystalline arrangement that forms due to the blend chain's and nanoparticles' interfacial adhesion causes the increase in $T_m$. Furthermore, when the quantity of $Co_3O_4$ NPs increases, the area under the melting peak diminishes. An increase in the amorphous phase and a decrease in the crystalline phase for the polymer mix correspond to a smaller peak area of $T_m$, which could be advantageous for anion transport (Wu et al. 2006). The pure blend and PNCs' decomposition temperature ($T_d$) is responsible for the second endothermic peak, which is located in the 350–450 °C temperature range. Table 2 also includes a list of $T_m$ and $T_d$ values. Increasing the $Co_3O_4$ content raises the $T_d$ values, suggesting that this nanofiller enhances the blend's thermal stability (Sayed 2020). The DSC and TGA results show that adjusting the $Co_3O_4$ doped ratio can modify the PEO/PVDF blend's stability and thermal characteristics. The percentage degree of crystallinity Xc (%) in the mix matrix of the produced PNCs films is determined by the area under the endothermic melting peak of the corresponding polymer quantities, which can be calculated using the following relationship (Charan et al. 2024):

$$XC = \left[\Delta H_m / \Delta H_m^*\right] \times 100 \ (\%) \tag{4}$$

where $\Delta H_m$ is the obtained melting enthalpy of the blended polymer component, which is equivalent to the area under the corresponding melting peak, and $\Delta H_m^*$ is the melting heat per unit mass of the PVDF assumed to be 100% crystalline, and it is approximated as 104.7 J/g (Hema et al. 2017). Table 2 summarizes the degree of crystallinity value. This table makes it evident that, in a pure mix system, the value of Xc falls as the amount of $Co_3O_4$ NPs increases. This is consistent with XRD findings and the ionic conductivity.

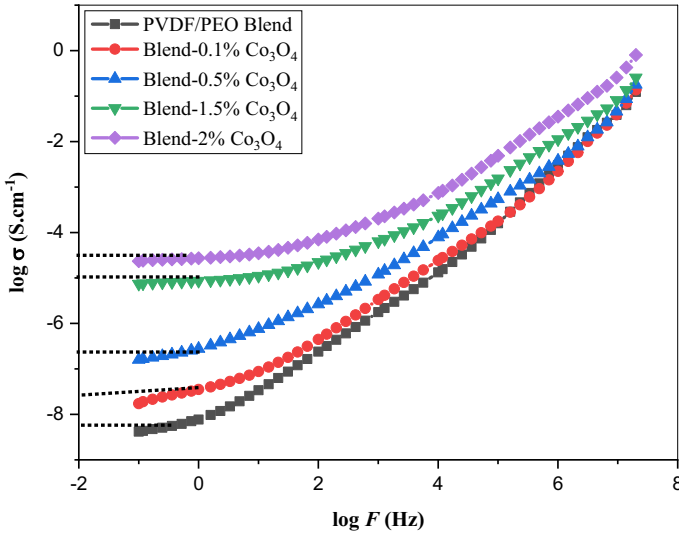| **Table 2** DSC data for pure PVDF/PEO and PNCs at different contents of $Co_3O_4$ NPs | Samples | $T_m$ (ºC) | $T_d$ (ºC) | $\Delta H_m$ (J/g) | Crystallinity, Xc (%) |
|---|---|---|---|---|---|
| | PVDF/PEO blend | 130 | 401 | 42.23 | 40.33 |
| | PVDF/PEO/0.1%$Co_3O_4$ | 133 | 407 | 39.33 | 37.56 |
| | PVDF/PEO/0.5%$Co_3O_4$ | 135 | 415 | 36.96 | 35.3 |
| | PVDF/PEO/1.5%$Co_3O_4$ | 140 | 420 | 33.59 | 32.08 |
| | PVDF/PEO/2%$Co_3O_4$ | 143 | 425 | 28.14 | 26.87 |

**Fig. 9** Frequency dependent conductivity of pure blend and PVDF/PEO-$Co_3O_4$ nanocomposites films

## 3.7 Study of AC conductivity

The AC conductivity was determined by utilizing the subsequent formula (El-Sayed et al. 2020):

$$\sigma_{AC} = 2\pi f\, \varepsilon_o\, \varepsilon'' \tag{5}$$

Figure 9 shows the relationship of conductivity the frequency. At RT, the frequency was adjusted within the range of 100Hz–7MHz. It is evident that the conductivity of the nanocomposite samples grows in tandem with the frequency and $Co_3O_4$ content. The improvement in conductivity occurs from interactions of the nanofiller with functional group of the PVDF/PEO blend. The polymer's band structure and chemical makeup have altered as a result of these interactions, and a charge-transfer complex (CTC) that improves the chain's flexibility has been created. Habeeb (2016) shows that for the PVDF/PEO blend, the AC electrical conductivity increases from $7.5 \times 10^{-6}$ $Scm^{-1}$ to $6.5 \times 10^{-4}$ $Scm^{-1}$ at 4 MHz when the nanofiller concentration increases. As the applied frequency rises, bonds in the PVDF/PEO start to rotate, and dielectric relaxation is brought on by the flexible polar groups present in polar bonds. Consequently, as frequency rises, electrical conductivity rises as well (El-Sayed et al. 2020). The $\sigma_{dc}$ value was calculated by measuring the junctions at f=0 and concluding the plateau regions to the Log $\sigma_{ac}$ axis. The dashed lines in Fig. 8 show this, and Table 1 lists the values that were achieved. Percolation happens when the $Co_3O_4$ NPs reach 2 weight percent, and the electrical conductivity rises to $6.5 \times 10^{-4}$ $Scm^{-1}$. The AC electrical conductivity that is dependent on frequency was explained by Singh et al. (2006):

$$\sigma_{AC} = A\omega^s \tag{6}$$

where, $s$ is the power-law exponent ($0 < s < 1$) and $A$ is constant. The degree of contact between the mobile ions is represented by this power-law, which is connected to the dynamics of hopping transit between states in the forbidden gap. The fluctuation of s

parameters with respect to $Co_3O_4$ NPs is shown in Table 1. This figure illustrates how the *s* values slightly dropped as the content of $Co_3O_4$ NPs grew, this indicates that an increase in the concentration of $Co_3O_4$ NPs causes a rise in conductivity.

### 3.8 Dielectric properties

The dielectric constant (ε′) and dielectric loss (ε″) of polymer electrolytes are critical factors that determine their suitability for energy storage applications. The dielectric responses of polymer nanocomposites are a powerful tool for studying ion dynamics (Bhavsar et al. 2022). The ε″ is related to conductance, which describes the energy required to align the dipoles, whereas the ε′ is related to capacitance, which defines dipole alignment or polarization. The ε′ and ε″ trend for pure PVDF/PEO and PVDF/PEO-$Co_3O_4$ nanocomposites at RT are shown in Fig. 10. It is evident from the dielectric plots that at higher frequencies, the ε′ and ε″ approaches a steady value and declines monotonically. For different frequencies, every composition exhibits the same dielectric behavior. The ε″ and ε′ are high at lower frequencies at first. At higher frequencies, the lowering of ε' and ε″ is caused by a limited dipole response to sudden changes in the field. The charging accumulation at the electrode–electrolyte interface is responsible for the lower frequency dispersion zone in the frequency-dependent conductivity plot (Alghamdi et al. 2022). The rapid reversal of the electric field at higher frequencies Fig. 9a, b limits ionic diffusion along the field axis due to insufficient time for significant displacement within a single cycle. Therefore, even in the case of field reversals, net ionic mobility becomes negligible (Morsi et al. 2019). As a result, for every sample, dielectric behavior diminishes with increasing frequency (Rajeh et al. 2019). When compared to pristine PVDF/PEO, the addition of nanofiller raises the ε′ and ε″ due to the characteristics of the composite material, which are influenced by the nature, concentration, and quantity of defects as well as the interfacial contact between the nanofiller and polymer (Albalawi et al. 2023; Alsalmah et al. 2023). The Maxwell–Wagner-Sillars (MWS) polarization effect is the reason why the energy storage capacity of the nanocomposites is more intense than that of the pure blend, as Fig. 9a makes clear. Because of the strong interfacial contacts and consequently stronger dielectric characteristics, the MWS effect polarization is maximal in 2%$Co_3O_4$-PVDF/PEO. Furthermore, the nanocomposite system's dielectric constant is improved because the displacement of charges in the areas where polymers and nanoparticles interface is sufficient to lower a tiny percentage of the applied signal frequency (Alharbi and Rajeh 2022; Al-Sagheer and Rajeh 2023). Additionally, it is noted that the addition of $Co_3O_4$ NPs causes an increase in the dielectric constant, which is explained by an increase in the number of mobile ions and, as a result, the ionic conductivity increase (Mazuki et al. 2020). Figure 11 shows the frequency variation of ε′ and ε″ for 2%$Co_3O_4$-PVDF/PEO nanocomposites film at various temperatures. It was discovered that as temperatures rise, so do the values of ε′ and ε″. The dipole is stationary at lower temperatures and cannot respond to an applied field. Raising the temperature causes the viscosity of the nanocomposite films to drop, giving them enough energy to readily orient when an externally applied field is applied, as a result, ε′ and ε″ rise. The activation energy barrier that prevents the electric dipoles from being oriented in the direction of the electric field is partially overcome by heating. Additionally, the chain's segmental motion and orientation are improved, as well as the motion of the free charge carriers (El-Gamal and Sayed 2019). For all films, these variables increase polarization and, by extension, ε′ and ε″. Similar outcomes were also reported for CMC/PVA-$Co_3O_4$ nanocomposites samples (Sayed and El-Gamal 2015).
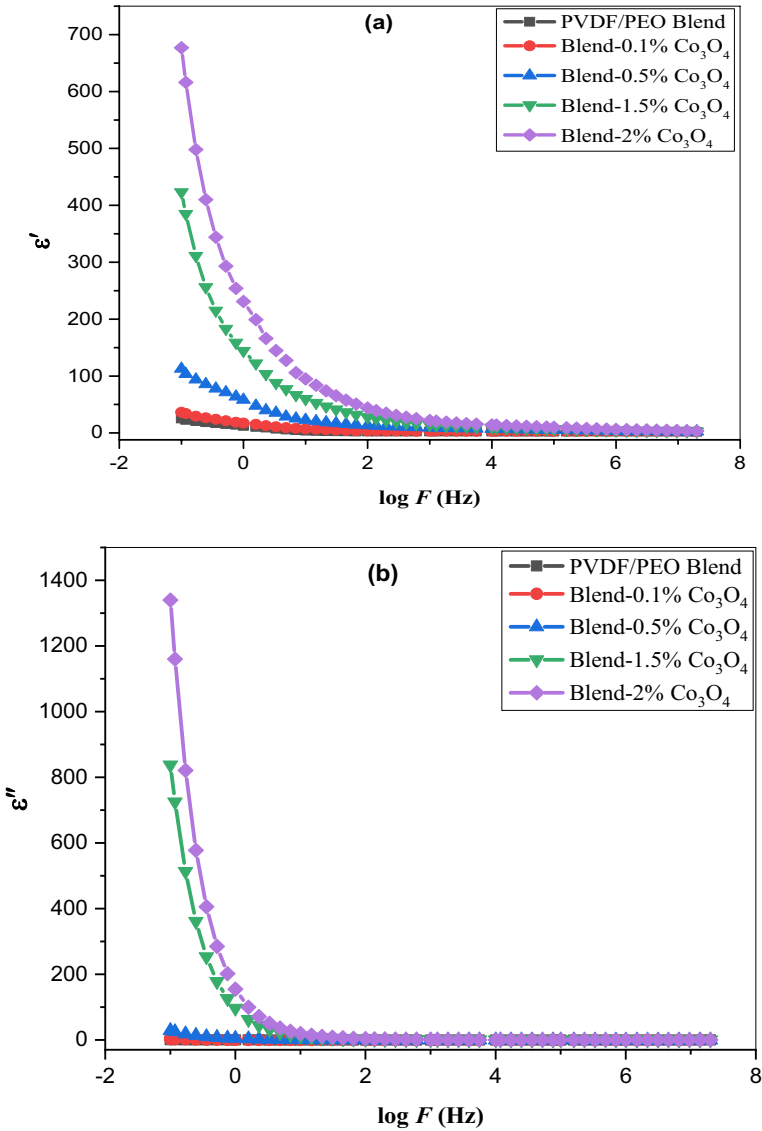
**Fig. 10** Dielectric permittivity **a** $\varepsilon'$ and **b** $\varepsilon''$ spectra for the pure blend and PVDF/PEO-Co$_3$O$_4$ nanocomposites films

## 4 Conclusions

Films of PVDF/PEO/Co$_3$O$_4$ polymer nanocomposites were made by solution casting method. XRD, FTIR, and SEM methods were used to get structural characterization data for the films. The semicrystalline structure of the PVDF/PEO blend film was demonstrated by the XRD patterns. The inclusion of Co$_3$O$_4$ NPs increases the amorphous nature and the good dispersion of nanoparticles in the polymer mix host is confirmed by the decreasing
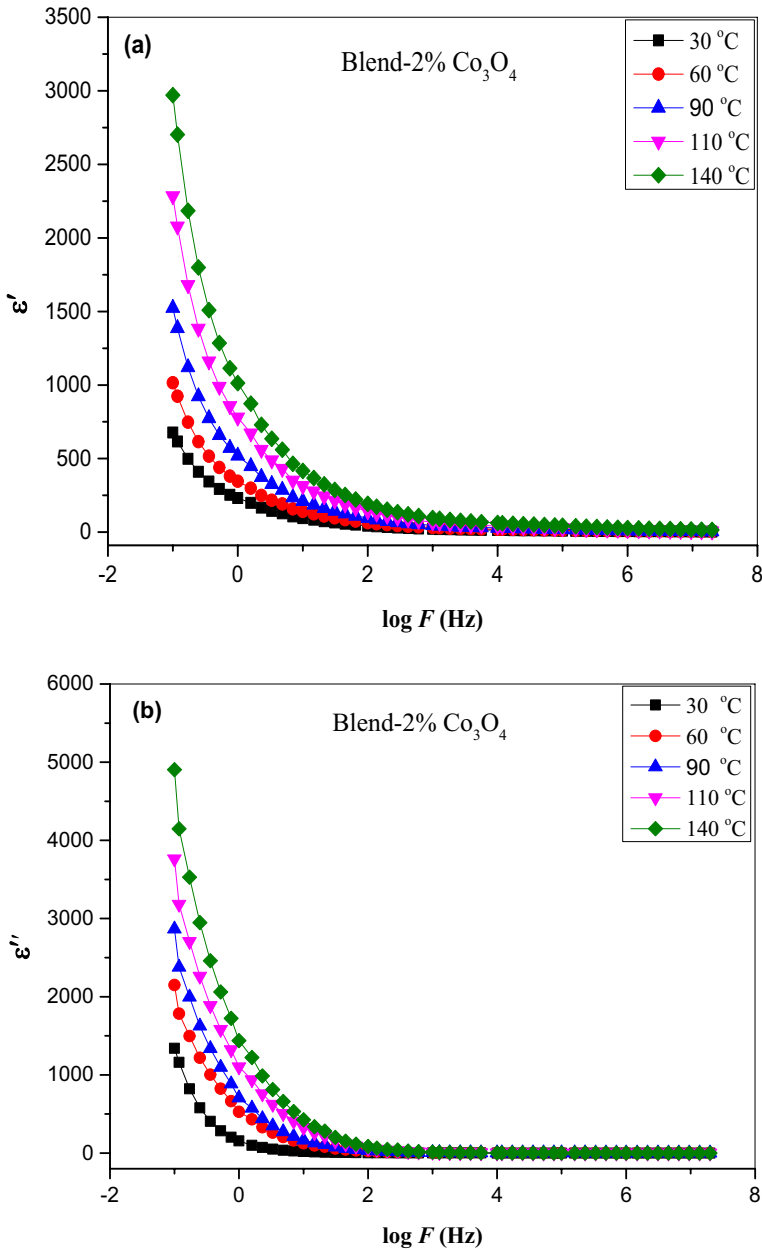
**Fig. 11** The dependence of the $\varepsilon'$ and $\varepsilon''$ for $2\%Co_3O_4$-PVDF/PEO on frequency at various temperatures

in the intensity of the crystalline peaks. FTIR spectra could demonstrate the intermolecular interaction between the blend's polar segments and $Co_3O_4$ nanoparticles. When the $Co_3O_4$ content increased, the optical results revealed reduce in the optical band gap and an increase in the Urbach energy gap. This was caused by an increase in the density of

localized states, which decreased bond accumulation. TGA data showed that the decomposition of the nanocomposite was less than that of pure PVDF/PEO, indicating an improvement in thermal stability. When the concentration of nanoparticles increased, so did the AC conductivity of PVDF/PEO loaded with $Co_3O_4$ NPs, which was higher than that of the pure PVDF/PEO. As the applied frequency was increased, both $\varepsilon'$ and $\varepsilon''$ decreased. In the higher frequency regions, the $\varepsilon'$ remained constant and increased as the quantity of $Co_3O_4$ ions increased. The enhanced $\varepsilon'$ of the produced samples are a result of the robust hydrogen bonding interactions between the $Co_3O_4$ ions and the polymer chains. We may conclude that the inclusion of $Co_3O_4$ NPs improves the thermal, structural, optical, and dielectric properties of PVDF/PEO. Ultimately, the special qualities of PVDF/PEO/$Co_3O_4$ nanocomposite films allow them to be applied in a variety of fields, including optoelectronics, electronics, and other flexible energy storage devices (i.e., electrochemical capacitors and batteries).

**Data availability** Data will be made available on request.

## Declarations

**Conflict of interest** The authors declare that they have no known competing financial interests or personal relationships that could have appeared to influence the work reported in this paper.

## References

Abdelaziz, M.: Investigations on optical and dielectric properties of PVDF/PMMA blend doped with mixed samarium and nickel chlorides. J. Mater. Sci. Mater. Electron. **24**, 2727–2736 (2013). https://doi.org/10.1007/s10854-013-1162-x

Abdelrazek, E.M., Hezma, A.M., El-khodary, A., Elzayat, A.M., Rajeh, A.: Modifying of structural, optical, thermal, and mechanical properties of PCL/PMMA biomaterial blend doped with MWCNTs as an application in materials science. J. Inorg. Organomet. Polym. Mater. **33**, 4117–4126 (2023)

Abdullah, O.G., Aziz, S.B., Rasheed, M.A.: Structural and optical characterization of PVA: KMnO4 based solid polymer electrolyte. Results Phys. **6**, 1103–1108 (2016). https://doi.org/10.1016/J.RINP.2016.11.050

Albalawi, H., Alharbi, E.M., Al-Sulami, A.I., Al-Qahtani, N., Farea, M.O., Rajeh, A.: Synthesis and characterization of sodium alginate/polyvinyl alcohol/zinc oxide/iron oxide nanocomposites for electrochemical applications. Polym. Compos. **44**, 1762–1771 (2023)

Alghamdi, H.M., Rajeh, A.: Synthesis of CoFe2O4/MWCNTs nanohybrid and its effect on the optical, thermal, and conductivity of PVA/CMC composite as an application in electrochemical devices. J. Inorg. Organomet. Polym. Mater. **32**, 1935–1949 (2022)

Alghamdi, H.M., Rajeh, A.: Comparative analysis of the structural, optical, mechanical, and electrical properties of PMMA/PU blend-based nanocomposites with $FeVO_4$ nanofiller for energy storage devices. Polym. Adv. Technol. **34**, 3711–3721 (2023a)

Alghamdi, H.M., Rajeh, A.: Study of the photoluminescence, optical, thermal, and electrical parameters of the Cs/PVP blend/zinc oxide nanorods films for energy storage devices. Polym. Test. **124**, 108093–108102 (2023b)

Alghamdi, H.M., Abutalib, M.M., Mannaa, M.A., Nur, O., Abdelrazek, E.M., Rajeh, A.: Modification and development of high bioactivities and environmentally safe polymer nanocomposites doped by Ni/ZnO nanohybrid for food packaging applications. J. Mater. Res. Technol. **19**, 3421–3432 (2022). https://doi.org/10.1016/J.JMRT.2022.06.077

Al-Gharram, M., AlZoubi, T.: Electrochemical synthesis of a novel hybrid nanocomposite based on $Co_3O_4$ nanoparticles embedded in PANI- camphor sulfonic Acid matrix for optoelectronic applications. Ceram. Int. **50**, 5473–5482 (2024)

Alharbi, E.M., Rajeh, A.: Tailoring the structural, optical, dielectric, and electrical properties of PEO/PVA blend using graphene nanoplates for energy storage devices. J. Mater. Sci. Mater. Electron. **33**, 22196–22207 (2022)

Almehmadi, S.J., Alruqi, A.B., Alsalmah, H.A., Farea, M.O., Masmali, N.A., Al-Sulami, A.I., Al-Ejji, M., Rajeh, A.: Improving the optical, photoluminescence, and electrical properties of PEO/NaAlg-WO3 nanocomposites for optoelectronic and nanodielectric applications. J. Mater. Res. Technol. **26**, 2310–2318 (2023). https://doi.org/10.1016/J.JMRT.2023.08.044

Alqarni, L.S., Alghamdi, A.M., Elamin, N.Y., Rajeh, A.: Enhancing the optical, electrical, dielectric properties and antimicrobial activity of chitosan/gelatin incorporated with Co-doped ZnO nanoparticles: nanocomposites for use in energy storage and food packaging. J. Mol. Struct. **1297**, 137011–137022 (2024). https://doi.org/10.1016/J.MOLSTRUC.2023.137011

Al-Sagheer, L.A.M., Rajeh, A.: Synthesis, characterization, electrical, and magnetic properties of polyvinyl alcohol/carboxymethyl cellulose blend doped with nickel ferrites nanoparticles for magneto-electronic devices. Polym. Compos. **44**, 7156–7169 (2023)

Alsalmah, H.A., Almehmadi, S.J., Farea, M.O., Alsulami, Q.A., Albalawi, H., Rajeh, A.: Hybrid GO/$TiO_2$ nanoparticles reinforced NaAlg/PVA blend: nanocomposites for high-performance energy storage devices. Polym. Adv. Technol. **34**, 2831–2840 (2023)

Alsalmah, H.A., et al.: Synthesis and characterization of PEG/CS-AgNO3 polymer nanocomposites for flexible optoelectronic and energy storage applications. Polym. Compos. **45**, 5164–5175 (2024a)

Alsalmah, H.A., Rajeh, A., Nur, O.: Optical, conductivity, dielectric, and magnetic properties of polymer nanocomposite based on PAM/cs matrix and ZnFe2O4 NPs for use in magneto-electronic and energy storage capacitor devices. Ceram. Int. **50**, 12167–12174 (2024b)

Al-Sulami, A.I., et al.: Nanocomposites comprising PVA/CMC matrix and CNTs/Fe2O3 nanohybrid: a comparative investigation of structural, optical, electrical, and dielectric properties as an application in advanced electrochemical and optoelectronic devices. Mater. Chem. Phys. **315**, 128971–128982 (2024)

Alsulami, Q.A., Rajeh, A.: Synthesis of the SWCNTs/TiO2 nanostructure and its effect study on the thermal, optical, and conductivity properties of the CMC/PEO blend. Results Phys. **28**, 104675–104686 (2021). https://doi.org/10.1016/J.RINP.2021.104675

Alsulami, Q.A., Rajeh, A.: Modification and development in the microstructure of PVA/CMC-GO/Fe3O4 nanocomposites films as an application in energy storage devices and magnetic electronics industry. Ceram. Int. **49**, 14399–14407 (2023)

Alzahrani, H.S., Al-Sulami, A.I., Alsulami, Q.A., Rajeh, A.: A systematic study of structural, conductivity, linear, and nonlinear optical properties of PEO/PVA-MWCNTs/ZnO nanocomposites films for optoelectronic applications. Opt. Mater. (amst) **133**, 112900–112911 (2022). https://doi.org/10.1016/J.OPTMAT.2022.112900

Appetecchi, G.B., Hassoun, J., Scrosati, B., Croce, F., Cassel, F., Salomon, M.: Hot-pressed, solvent-free, nanocomposite, PEO-based electrolyte membranes: II. All solid-state Li/LiFePO4 polymer batteries. J. Power. Sources **124**, 246–253 (2003)

Baskaran, R., Selvasekarapandian, S., Kuwata, N., Kawamura, J., Hattori, T.: ac impedance, DSC and FT-IR investigations on (x)PVAc–(1–x)PVdF blends with LiClO4. Mater. Chem. Phys. **98**, 55–61 (2006). https://doi.org/10.1016/J.MATCHEMPHYS.2005.08.063

Bhatt, A.S., Bhat, D.K.: Crystallinity, magnetic and electrochemical studies of PVDF/$Co_3O_4$ polymer electrolyte. Mater. Sci. Eng. B **177**, 127–131 (2012). https://doi.org/10.1016/J.MSEB.2011.09.036

Bhavsar, S., Patel, G.B., Singh, B., Singh, F., Singh, N.L.: A comparative study on gamma and carbon ion irradiations induced modification in structural and electrical properties of PVA/H3PO4/SiO2 nanocomposite polymer electrolyte. Radiat. Phys. Chem. **192**, 109916 (2022). https://doi.org/10.1016/J.RADPHYSCHEM.2021.109916

Boranna, M.P., Patil, P.S., Gummagol, N.B., Ravikumar, H.B.: Positron lifetime and third-order nonlinear optical studies of P(St-co-MMA)/NiO polymer nanocomposites. Opt. Mater. (amst). **140**, 113843 (2023). https://doi.org/10.1016/J.OPTMAT.2023.113843

Charan, C.P., Sengwa, R.J., Saraswat, M.: Synergistic effect of polymer blend compositions on the structural, thermal, optical, and broadband dielectric properties of P(VDF-HFP)/PEO/ZnO polymer nanocomposites. Chem. Phys. Impact. **8**, 100410 (2024)

Choudhary, S., Sengwa, R.J.: ZnO nanoparticles dispersed PVA–PVP blend matrix based high performance flexible nanodielectrics for multifunctional microelectronic devices. Curr. Appl. Phys. **18**, 1041–1058 (2018). https://doi.org/10.1016/J.CAP.2018.05.023

Chu, R., et al.: Preparation and properties comparison of ZIF-67/PVDF and SiCNWs/PVDF composites for energy storage. J. Mater. Sci. Mater. Electron. **34**(5), 347 (2023)

Dallaev, R., Pisarenko, T., Sobola, D., Orudzhev, F., Ramazanov, S., Trčka, T.: Brief review of PVDF properties and applications potential. Polymers **14**, 4793 (2022)

Deeba, F., Gupta, A.K., Kulshrestha, V., Bafna, M., Jain, A.: Analysing the dielectric properties of ZnO doped PVDF/PMMA blend composite. J. Mater. Sci. Mater. Electron. **33**, 23703–23713 (2022). https://doi.org/10.1007/s10854-022-09129-1

Dey, A., Ghoshal, T., Karan, S., De, S.K.: Size effect of cubic ZrO2 nanoparticles on ionic conductivity of polyethylene oxide-based composite. J. Appl. Phys. **110** (2011)

Dhatarwal, P., Sengwa, R.J.: Synergistic effects of salt concentration and polymer blend composition on the crystal phases, dielectric relaxation, and ion conduction in PVDF/PEO/LiCF3SO3 solid polymer electrolytes. Ionics (kiel) **26**, 2259–2275 (2020a)

Dhatarwal, P., Sengwa, R.J.: Tunable β-phase crystals, degree of crystallinity, and dielectric properties of three-phase PVDF/PEO/SiO2 hybrid polymer nanocomposites. Mater. Res. Bull. **129**, 110901 (2020b). https://doi.org/10.1016/J.MATERRESBULL.2020.110901

Dhatarwal, P., Sengwa, R.J.: Crystalline phases thermal behaviour, optical energy band gap, and broadband radio wave frequency dielectric properties of PEO/PVDF blend films. Macromol. Res. **30**, 460–469 (2022). https://doi.org/10.1007/s13233-022-0052-6

El Sayed, A.M.: Synthesis, optical, thermal, electric properties and impedance spectroscopy studies on P(VC-MMA) of optimized thickness and reinforced with MWCNTs. Results Phys. **17**, 103025 (2020). https://doi.org/10.1016/J.RINP.2020.103025

El Sayed, A.M., El-Gamal, S.: Synthesis and investigation of the electrical and dielectric properties of Co3O4/(CMC+PVA) nanocomposite films. J. Polym. Res. **22**, 97 (2015)

El-Gamal, S., El Sayed, A.M.: Physical properties of the organic polymeric blend (PVA/PAM) modified with MgO nanofillers. J. Compos. Mater. **53**, 2831–2847 (2019)

El-Sayed, F., Mohammed, M.I., Yahia, I.S.: Discussions on the film design and mechanical properties of Y3+/PVA polymeric composite films: enhancement of the electrical conductivity and dielectric properties. J. Mater. Sci. Mater. Electron. **31**, 10408–10421 (2020)

Farhadi, S., Javanmard, M., Nadri, G.: Characterization of cobalt oxide nanoparticles prepared by the thermal decomposition of [Co(NH3)5(H2O)](NO3)3 complex and study of their photocatalytic activity. Acta Chim. Slovaca. **2**, 335–343 (2016)

Formela, K., Marć, M., Namieśnik, J., Zabiegała, B.: The estimation of total volatile organic compounds emissions generated from peroxide-cured natural rubber/polycaprolactone blends. Microchem. J. **127**, 30–35 (2016). https://doi.org/10.1016/J.MICROC.2016.02.001

Habeeb, M.A.: Enhancement of dielectric and optical properties of (PVA-PAA-PEG) blend-yttrium oxide nanoparticle for biomedical applications, mater. Focus **5**, 550–555 (2016). https://doi.org/10.1166/mat.2016.1359

Hema, M., Selvasekarapandian, S., Arunkumar, D., Sakunthala, A., Nithya, H.: FTIR, XRD and ac impedance spectroscopic study on PVA based polymer electrolyte doped with NH4X (X = Cl, Br, I). J. Non Cryst. Solids **355**, 84–90 (2009)

Hema, M., Tamilselvi, P., Pandaram, P.: Conductivity enhancement in SiO2 doped PVA: PVDF nanocomposite polymer electrolyte by gamma ray irradiation. Nucl. Instr. Methods Phys. Res. Sect B Beam Interact. Mater. Atoms. **403**, 13–20 (2017)

Kacem, E., Althobaiti, H.A., Al-Ejji, M., Bader, N., Abed, A., Rajeh, A.: Structural, optical, and thermal studies of Poly(vinylidene fluoride-co-hexafluoropropylene) and Polyvinylpyrrolidone composite doped Ag/ZnO mixed nanoparticles for flexible optoelectronic devices. Opt. Mater. (amst) **146**, 114560 (2023)

Kim, M., Lee, L., Jung, Y., Kim, S.: Study on Ion conductivity and crystallinity of composite polymer electrolytes based on Poly(ethylene oxide)/Poly(acrylonitrile) containing nano-sized Al2O3 Fillers. J. Nanosci. Nanotechnol. **13**, 7865–7869 (2013)

Kułek, J., Szafraniak, I., Hilczer, B., Połomska, M.: Dielectric and pyroelectric response of PVDF loaded with BaTiO3 obtained by mechanosynthesis. J. Non Cryst. Solids **353**, 4448–4452 (2007). https://doi.org/10.1016/J.JNONCRYSOL.2007.02.077

La Monaca, A., De Giorgio, F., Focarete, M.L., Fabiani, D., Zaccaria, M., Arbizzani, C.: Polyvinylidene difluoride-polyethyleneoxide blends for electrospun separators in Li-Ion Batteries. J. Electrochem. Soc. **164**, A6431–A6439 (2017)

Long, L., Wang, S., Xiao, M., Meng, Y.: Polymer electrolytes for lithium polymer batteries. J. Mater. Chem. a. **4**, 10038–10069 (2016). https://doi.org/10.1039/C6TA02621D

Ma, L., Fan, H., Wei, X., Chen, S., Hu, Q., Liu, Y., Zhi, C., Lu, W., Zapien, J.A., Huang, H.: Towards high areal capacitance, rate capability, and tailorable supercapacitors: $Co_3O_4$ @polypyrrole core–shell nanorod bundle array electrodes. J. Mater. Chem. a. **6**, 19058–19065 (2018). https://doi.org/10.1039/C8TA07477A

Mazuki, N.F., Abdul Majeed, A.P.P., Nagao, Y., Samsudin, A.S.: Studies on ionics conduction properties of modification CMC-PVA based polymer blend electrolytes via impedance approach. Polym. Test. **81**, 106234 (2020)

Meng, Q., Li, W., Zheng, Y., Zhang, Z.: Effect of poly(methyl methacrylate) addition on the dielectric and energy storage properties of poly(vinylidene fluoride). J. Appl. Polym. Sci. **116**, 2674–2684 (2010). https://doi.org/10.1002/app.31777

Mohammed, M.I., Fouad, S.S., Mehta, N.: Dielectric relaxation and thermally activated a.c. conduction in (PVDF)/(rGO) nano-composites: role of rGO over different fillers. J. Mater. Sci. Mater. Electron. **29**, 18271–18281 (2018). https://doi.org/10.1007/s10854-018-9941-z

Morsi, M.A., Rajeh, A., Al-Muntaser, A.A.: Reinforcement of the optical, thermal and electrical properties of PEO based on MWCNTs/Au hybrid fillers: nanodielectric materials for organoelectronic devices. Compos. Part B Eng. **173**, 106957 (2019)

Mukherjee, A., Dasgupta Ghosh, B.: Synthesis of functionalized ZnO nanoflake loaded polyvinylidene fluoride composites with enhanced energy storage properties. Polym. Compos. **44**, 2488–2499 (2023). https://doi.org/10.1002/pc.27258

Ningaraju, S., Ravikumar, H.B.: Ionic and electronic transport in PSF/NiO and PSF/TiO2 polymer nanocomposites: a positron lifetime study. Solid State Ionics **310**, 81–94 (2017). https://doi.org/10.1016/J.SSI.2017.08.009

Ouyang, Z.-W., Chen, E.-C., Wu, T.-M.: Thermal stability and magnetic properties of polyvinylidene fluoride/magnetite nanocomposites. Materials (basel) **8**, 4553–4564 (2015). https://doi.org/10.3390/ma8074553

Panwar, V., Cha, K., Park, J.-O., Park, S.: High actuation response of PVDF/PVP/PSSA based ionic polymer metal composites actuator. Sensors Actuators B Chem. **161**, 460–470 (2012). https://doi.org/10.1016/J.SNB.2011.10.062

Patla, S.K., Ray, R., Asokan, K., Karmakar, S.: Investigation of ionic conduction in PEO–PVDF based blend polymer electrolytes. J. Appl. Phys. **123**, 125102 (2018)

Pradeepa, P., Edwin Raj, S., Sowmya, G., Kalaiselvimary, J., Ramesh Prabhu, M.: Optimization of hybrid polymer electrolytes with the effect of lithium salt concentration in PEO/PVdF-HFP blends. Mater. Sci. Eng. B **205**, 6–17 (2016)

Prasanth, R., Shubha, N., Hng, H.H., Srinivasan, M.: Effect of poly(ethylene oxide) on ionic conductivity and electrochemical properties of poly(vinylidenefluoride) based polymer gel electrolytes prepared by electrospinning for lithium ion batteries. J. Power. Sources **245**, 283–291 (2014). https://doi.org/10.1016/J.JPOWSOUR.2013.05.178

Ragab, H.M., Diab, N.S., Khaled, A.M., Al Ojeery, A., Al-Hakimi, A.N., Farea, M.O.: Incorporating hybrid $Ag/Co_2O_3$ nanofillers into PVP/CS blends for multifunctional optoelectronic and nanodielectric applications. Ceram. Int. **50**, 1254–1262 (2024)

Rajabzadeh, S., Maruyama, T., Ohmukai, Y., Sotani, T., Matsuyama, H.: Preparation of PVDF/PMMA blend hollow fiber membrane via thermally induced phase separation (TIPS) method. Sep. Purif. Technol. **66**, 76–83 (2009)

Rajeh, A., Morsi, M.A., Elashmawi, I.S.: Enhancement of spectroscopic, thermal, electrical and morphological properties of polyethylene oxide/carboxymethyl cellulose blends: Combined FT-IR/DFT. Vacuum **159**, 430–440 (2019)

Rajeh, A., Althobaiti, H.A., Almehmadi, S.J., Alsalmah, H.A., Masmali, N.A., Al-Sulami, A.I., Al-Ejji, M.: Alteration in the structural, optical, thermal, electrical, and dielectric properties of PMMA/PVDF blend by Incorporation of Ni/ZnO nanohybrid for optoelectronic and energy storage devices. J. Inorg. Organomet. Polym. Mater. **34**, 1221–1231 (2023)

Ravisankar, M.S., Pramod, K., Gangineni, R.B.: Effect of the top electrode on local piezoelectric and the ferroelectric response of PVDF thin films in PVDF/Au/Si and Ag/PVDF/Au/Si multilayers. Appl. Phys. A **129**(2), 146 (2023)

Ren, X., Fan, H., Ma, J., Wang, C., Zhang, M., Zhao, N.: Hierarchical $Co_3O_4$/PANI hollow nanocages: synthesis and application for electrode materials of supercapacitors. Appl. Surf. Sci. **441**, 194–203 (2018). https://doi.org/10.1016/J.APSUSC.2018.02.013

Saeed, S.Y., Mazhar, K., Raees, L., Mukhtiar, A., Khan, F., Khan, M.: Green synthesis of cobalt oxide nanoparticles using roots extract of Ziziphus Oxyphylla Edgew its characterization and antibacterial activity. Mater. Res. Express. **9**, 105001 (2022)

Sengwa, R.J., Dhatarwal, P.: Nanofiller concentration-dependent appreciably tailorable and multifunctional properties of (PVP/PVA)/SnO2 nanocomposites for advanced flexible device technologies. J. Mater. Sci. Mater. Electron. **32**, 9661–9674 (2021). https://doi.org/10.1007/s10854-021-05627-w

Sengwa, R.J., Dhatarwal, P.: Toward multifunctionality of PEO/PMMA/MMT hybrid polymer nanocomposites: promising morphological, nanostructural, thermal, broadband dielectric, and optical properties. J. Phys. Chem. Solids **166**, 110708 (2022)

Sengwa, R.J., Choudhary, S., Dhatarwal, P.: Nonlinear optical and dielectric properties of TiO2 nanoparticles incorporated PEO/PVP blend matrix based multifunctional polymer nanocomposites. J. Mater. Sci. Mater. Electron. **30**, 12275–12294 (2019). https://doi.org/10.1007/s10854-019-01587-4

Sengwa, R.J., Dhatarwal, P., Choudhary, S.: A comparative study of different metal oxide nanoparticles dispersed PVDF/PEO blend matrix-based advanced multifunctional nanodielectrics for flexible electronic devices. Mater. Today Commun. **25**, 101380 (2020)

Sengwa, R.J., Kumar, N., Saraswat, M.: Morphological, structural, optical, broadband frequency range dielectric and electrical properties of PVDF/PMMA/BaTiO$_3$ nanocomposites for futuristic microelectronic and optoelectronic technologies. Mater. Today Commun. **35**, 105625 (2023). https://doi.org/10.1016/J.MTCOMM.2023.105625

Shen, Y.J., Reddy, M.J., Chu, P.P.: Porous PVDF with LiClO4 complex as 'solid' and 'wet' polymer electrolyte. Solid State Ionics **175**, 747–750 (2004)

Singh, R., Kumar, J., Singh, R.K., Kaur, A., Sinha, R.D.P., Gupta, N.P.: Low frequency ac conduction and dielectric relaxation behavior of solution grown and uniaxially stretched poly(vinylidene fluoride) films. Polymer **47**, 5919–5928 (2006)

Wan, J., Xie, J., Mackanic, D.G., Burke, W., Bao, Z., Cui, Y.: Status, promises, and challenges of nanocomposite solid-state electrolytes for safe and high performance lithium batteries. Mater. Today Nano **4**, 1–16 (2018)

Wan, L., Tian, W., Li, N., Chen, D., Xu, Q., Li, H., He, J., Lu, J.: Hydrophilic porous PVDF membrane embedded with BaTiO3 featuring controlled oxygen vacancies for piezocatalytic water cleaning. Nano Energy **94**, 106930 (2022)

Wang, Y.-J., Kim, D.: Crystallinity, morphology, mechanical properties and conductivity study of in situ formed PVdF/LiClO4/TiO2 nanocomposite polymer electrolytes. Electrochim. Acta **52**, 3181–3189 (2007)

Wang, Q., Wu, C., LaChance, A.M., Zhou, J., Gao, Y., Zhang, Y., Sun, L., Cao, Y., Liang, X.: Interfacial polarization suppression of P(VDF-HFP) film through 2D montmorillonite nanosheets coating. Prog. Org. Coatings. **172**, 107119 (2022)

Wu, G.M., Lin, S.J., Yang, C.C.: Preparation and characterization of PVA/PAA membranes for solid polymer electrolytes. J. Memb. Sci. **275**, 127–133 (2006)

Xi, J., Qiu, X., Li, J., Tang, X., Zhu, W., Chen, L.: PVDF–PEO blends based microporous polymer electrolyte: effect of PEO on pore configurations and ionic conductivity. J. Power. Sources **157**, 501–506 (2006). https://doi.org/10.1016/J.JPOWSOUR.2005.08.009

Xia, J., Zheng, Z., Guo, Y.: Mechanically and electrically robust, electro-spun PVDF/PMMA blend films for durable triboelectric nanogenerators. Compos. Part A Appl. Sci. Manuf. **157**, 106914 (2022). https://doi.org/10.1016/J.COMPOSITESA.2022.106914

Ye, L.Y., Liu, Q.L., Zhang, Q.G., Zhu, A.M., Zhou, G.B.: Pervaporation characteristics and structure of poly(vinyl alcohol)/poly(ethylene glycol)/tetraethoxysilane hybrid membranes. J. Appl. Polym. Sci. **105**, 3640–3648 (2007)

Zhang, M., Xu, Y., Fan, H., Zhao, N., Yan, B., Wang, C., Ma, J., Yadav, A.K., Zhang, W., Du, Z., Zheng, X., Li, M., Dong, G., Wang, W.: In situ synthesis of 3D Co@Co$_3$O$_4$ nanosheet arrays for hybrid supercapacitors with ultra-high rate performance. J. Alloys Compd. **826**, 154115 (2020). https://doi.org/10.1016/J.JALLCOM.2020.154115

## Authors and Affiliations

**Ebtesam M. Alharbi[1] · A. Rajeh[2]**

✉ A. Rajeh
  a.rajeh88@yahoo.com

[1]    College of Science, Department of Physical Sciences, University of Jeddah, Jeddah, Saudi Arabia

[2]    Physics Department, Faculty of Applied Science, Sa'adah University, Sana'a, Yemen